Available online at www.sciencedirect.com

SciVerse ScienceDirect

Ceramics International 38 (2012) 6723–6728

CERAMICS INTERNATIONAL

www.elsevier.com/locate/ceramint

Effects of Al_2O_3 addition on the microstructure and microwave dielectric properties of $Ba_4Nd_{9.33}Ti_{18}O_{54}$ ceramics

Xiaogang Yao*, Huixing Lin, Xiangyu Zhao, Wei Chen, Lan Luo

Information Materials and Devices Research Center, Shanghai Institute of Ceramics, Chinese Academy of Science, 1295 Dingxi Road, Shanghai 200050, PR China

Received 31 March 2012; received in revised form 21 May 2012; accepted 23 May 2012
Available online 29 May 2012

Abstract

$Ba_4Nd_{9.33}Ti_{18}O_{54} \cdot x$ wt%Al_2O_3 (BNT-A) ceramics ($x=0$, 0.5, 1.0, 1.5, 2.0, 2.5) were prepared by the conventional solid state reaction. The effects of Al_2O_3 on the microstructure and microwave dielectric properties of $Ba_4Nd_{9.33}Ti_{18}O_{54}$ (BNT) ceramics were investigated. X-ray diffraction and backscatter electronic images showed that the Al_2O_3 additive gave rise to a second phase $BaAl_2Ti_5O_{14}$ (BAT). The formation mechanism and grain growth of the BAT phase were first discussed. Dielectric property test revealed that the Al_2O_3 additive had improved the dielectric properties of the BNT ceramics: increased the $Q \times f$ value from 8270 to 12,180 GHz and decreased the τ_f value from 53.4 to 11.2 ppm/°C. A BNT-A ceramic with excellent dielectric properties: $\varepsilon_r=70.2$, $Q \times f=12{,}180$ GHz, $\tau_f=20$ ppm/°C was obtained with 2.0 wt% Al_2O_3 added after sintering at 1320 °C for 4 h.

Keywords: A. Sintering; C. Dielectric properties; Ceramics; Microstructure

1. Introduction

The rapid progress for miniaturization in any hand-held communication application provides a continuing driving force for the discovery and development of increasingly sophisticated materials to perform the same or improved function with decreased size and weight [1]. New or improved dielectric ceramics with high permittivity (ε_r), high quality factor value ($Q \times f$) and low temperature coefficient of resonant frequency (τ_f) are playing a key role to meet the specifications of the current and future communication systems [2,3].

As a member of $Ba_{6-3x}R_{8+2x}Ti_{18}O_{54}$ (BRT, R = La, Pr, Nd, Sm), the high permittivity solid solution family, $Ba_4Nd_{9.33}Ti_{18}O_{54}$ ($x=2/3$) ceramic exhibits excellent dielectric constant near 85 [4–6]. However, the relatively low $Q \times f$ value about 8200 GHz and high τ_f of 55 ppm/°C as well as a sintering temperature (T_s) higher than 1380 °C restrict its commercial application. Much work has been done to improve the $Q \times f$ and τ_f values and lower the sintering temperature. Nagatomo et al. [7] reported that the substitution of Ba^{2+} and Nd^{3+} by Sr^{2+} and Y^{3+} could improve the $Q \times f$ value below the solid solubility limit of Sr^{2+}. Zhu et al. [8] reported that the $Q \times f$ value of $Ba_{4.2}Nd_{9.2}Ti_{18}O_{54}$ ceramic was increased from 7100 GHz to 11,400 GHz by adding 10 wt% $NdAlO_3$. Cheng et al. [9] and Zheng and Reaney [10] attached their attentions on the low temperature sintering of BNT ceramics by adding either ZnO powder or BBZS (Bi_2O_3–B_2O_3–ZnO–SiO_2) glass as sintering aid. Both of them significantly reduced the sintering temperature but inevitably increased the dielectric loss.

In our previous work, Al_2O_3 was proved to improve the Qf values of $Ba_{4.2}Sm_{9.2}Ti_{18}O_{54}$ ceramics effectively [11]. Given the similar composition, Al_2O_3 was again added into the BNT system in the present work. Special attention should be paid to the composition of $Ba_4Nd_{9.33}Ti_{18}O_{54}$, which has the lowest dielectric loss in BNT system as reported by Ohsato [12]. The effects of Al_2O_3 additive on the microstructure and microwave dielectric properties of BNT ceramics were investigated systematically.

*Corresponding author. Tel.: +86 21 5241 4112; fax: +86 21 5241 3903.
E-mail address: rockyao@student.sic.ac.cn (X. Yao).

0272-8842/$36.00
http://dx.doi.org/10.1016/j.ceramint.2012.05.063

2. Experimental procedure

The BNT ceramic powders were prepared according to the desired stoichiometry of $Ba_4Nd_{9.33}Ti_{18}O_{54}$ by mixing the chemical grade starting materials $BaCO_3$ (99.9%), Nd_2O_3 (99.9%) and TiO_2 (99.9%). After ground in deionized water with ZrO_2 balls for 24 h, the mixture was dried and then calcined at 1150 °C in air for 3 h.

Six BNT-A samples were prepared by adding 0, 0.5, 1.0, 1.5, 2.0 and 2.5 wt% of Al_2O_3 into the calcined BNT ceramic powders and noted as A00, A05, A10, A15, A20 and A25, respectively. The powders were milled for 24 h, dried at 120 °C and granulated with polyvinyl alcohol (PVA). The granules were preformed and then sintered at 1300∼1400 °C in air for 4 h with a heating rate of 5 °C/min.

The bulk densities of the BNT-A ceramics were measured by the Archimedes method. The crystalline phase was identified using a Rigaku D/max 2550V X-ray diffractometer with a conventional Cu-Kα radiation in the range of 10∼70° with a step size of 0.02°. The microstructure of the BNT-A ceramics was examined by a Hitachi S-4800 field emission scanning electron microscope. The method developed by Hakki and Coleman [13] was used to measure the microwave dielectric properties of the polished BNT-A samples. The testing was in the TE_{011} mode of an Agilent E8363A PNA series network analyzer with a frequency ranges from 3 to 4 GHz. τ_f was tested in the temperature range from 20 to 80 °C and calculated by noting the change in resonant frequency as:

$$\tau_f = (f_2\text{-}f_1)/60f_1 \quad (1)$$

here f_1 and f_2 represent the resonant frequencies at 20 and 80 °C, respectively.

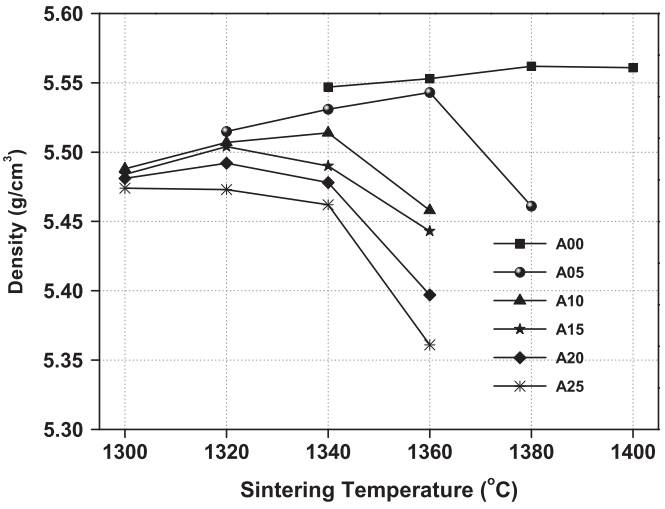

Fig. 1. Relationship between the bulk density of the BNT-A ceramics and the sintering temperature.

Table 1
Sintering temperature and density of $Ba_4Nd_{9.33}Ti_{18}O_{54}$ ceramics doped with different amounts of Al_2O_3.

x wt%	Sample	OST (°C)	Bulk density (g/cm^3)
0.0	A00	1380	5.562
0.5	A05	1360	5.543
1.0	A10	1340	5.514
1.5	A15	1320	5.504
2.0	A20	1320	5.492
2.5	A25	1300	5.474

3. Results and discussion

3.1. Density

Fig. 1 shows the bulk density of the BNT-A ceramics as a function of the sintering temperature. The density of the BNT-A ceramics decreases with the increasing amount of Al_2O_3. In addition, the optimum sintering temperature (OST), at which the density reaching the maximum value, decreases from 1380 °C of A00 to 1300 °C of A25, as listed in Table 1. According to the subsequent analysis, the monotonous decreases of the bulk density and the OST have a direct correlation with the formation of $BaAl_2Ti_5O_{14}$

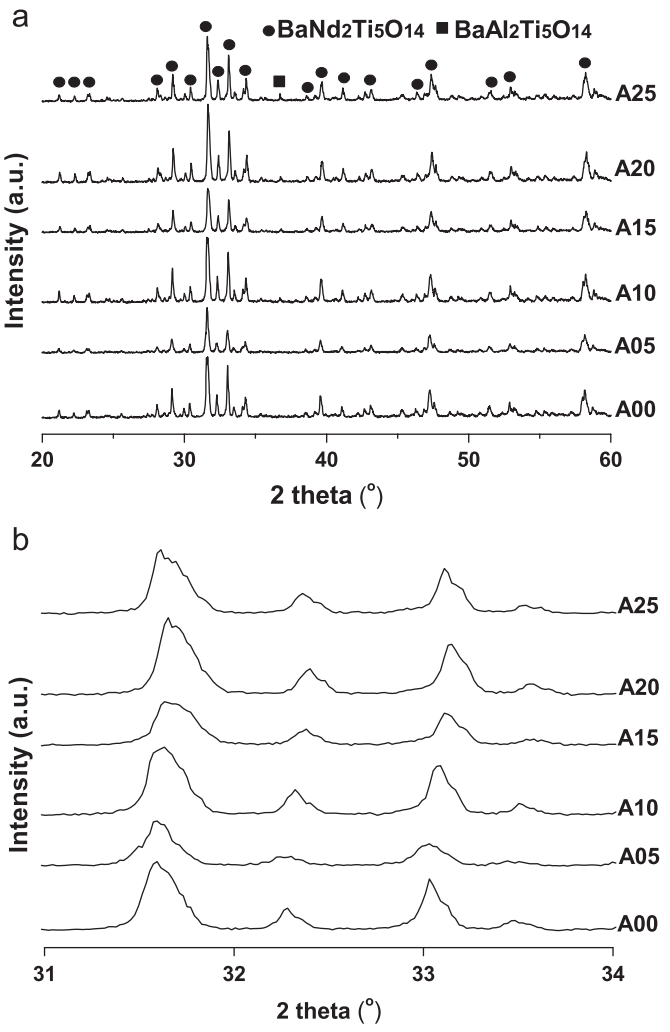

Fig. 2. XRD patterns of the BNT-A ceramic powders sintered at the OST for 4 h: (a) the whole diffraction area, (b) partial diffraction area enlarged.

(see Section 3.2 and 3.3), with a much lower density of 4.33 g/cm^3 [14].

3.2. Crystalline phase

Fig. 2a shows the powder X-ray diffraction patterns of BNT-A ceramics sintered at the optimum T_s for 4 h. The main crystalline phase $BaNd_2Ti_5O_{14}$ (JCPDS Card No. 33-0166) is identified and a minor second phase $BaAl_2Ti_5O_{14}$ (JCPDS Card No. 29-0146) appears when the amount of Al_2O_3 reaches 1.0 wt%. Furthermore, it is shown in Fig. 2b that the diffraction peaks of the $BaNd_2Ti_5O_{14}$ phase shift slightly toward higher 2θ degree values with the increasing x value from 0.5 to 2.0 wt%. Thus, according to the Bragg's law, we could deduce that the lattice parameters of the BNT structure have decreased.

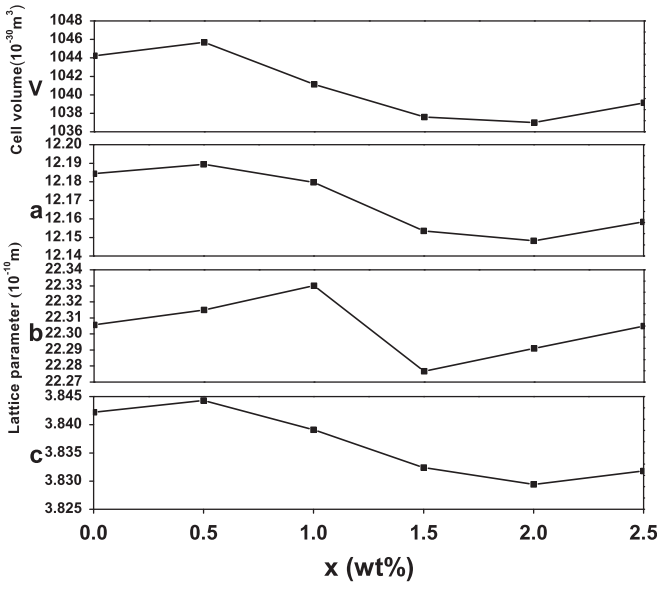

Fig. 3. Changes in lattice parameters and cell volume of the BNT structure with the increasing amount of Al_2O_3.

Fig. 3 shows the changes in lattice parameters and cell volume of the BNT crystal structure with the increasing amount of Al_2O_3. As we can see, the lattice parameters a, c and cell volume V shows the same variation trend: decreasing with the x value increased from 0.5 to 2.0. Two factors are believed to cause the contraction of the crystal structure. One is the substitution of Ti^{4+} in oxygen octahedron by smaller Al^{3+} [15] in the complex perovskite structure. The other is the deviation of Ba from the $Ba_4Nd_{9.33}Ti_{18}O_{54}$ solid solution to form $BaAl_2Ti_5O_{14}$ with Al_2O_3 and TiO_2. The decrease stops at $x=2.0$, which may suggest that the upper limit of Ti substituted by Al is near 2.0 wt%.

3.3. Microstructure

Fig. 4 shows the backscatter electronic images of the BNT ceramics doped with different amounts of Al_2O_3 and sintered at the optimum T_s for 4 h. No significant changes in grain shape or size of the main crystalline phase BNT are found in all the samples. However, more than one phase is observed in all the six samples. Table 2 shows the EDS analysis results of all the additional phases in each BNT-A sample, marked as A to F accordingly. The surrounding circle reveals the target range of EDS equipment. It is recognized, according to Table 2, that undoped BNT ceramic contains minor $BaTi_4O_9$ phase and the residual TiO_2 phase. With the increasing

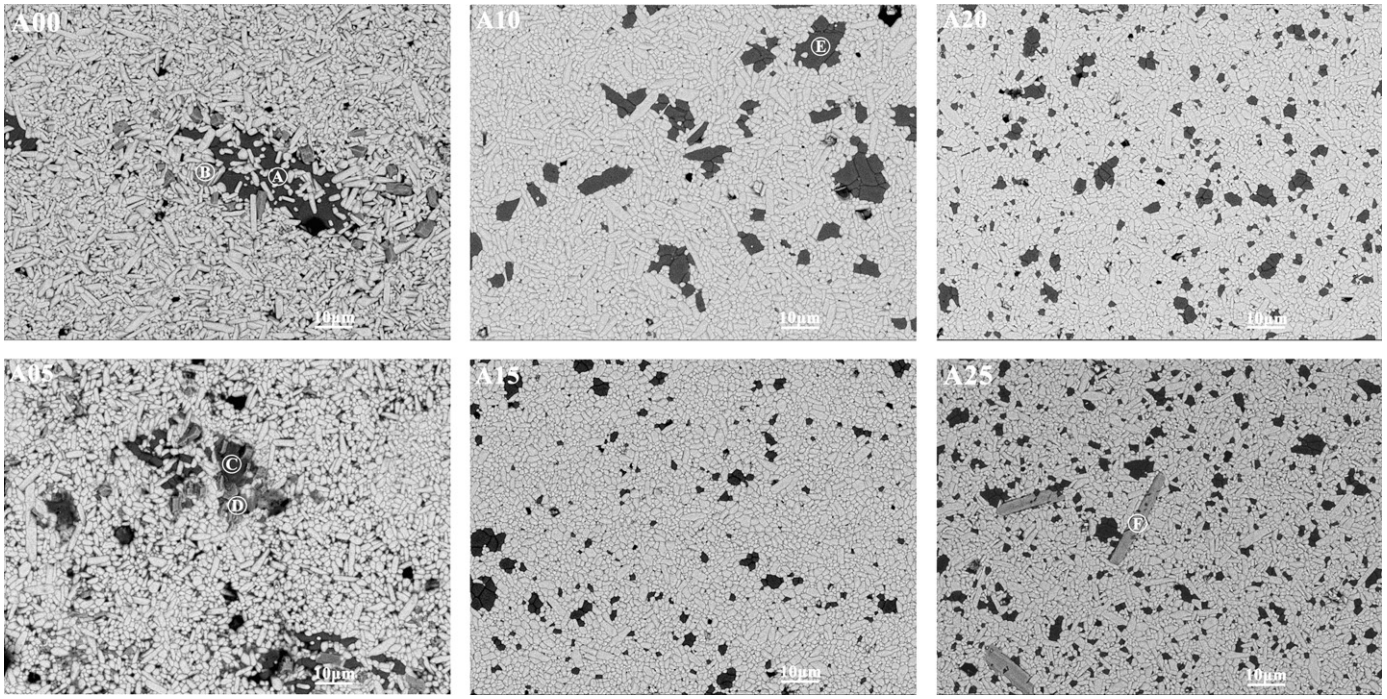

Fig. 4. Backscatter electronic (BSE) images of the BNT-A ceramics sintered at the optimum T_s for 4 h.

amount of Al_2O_3, $BaTi_4O_9$ and TiO_2 phases disappear and $BaAl_2Ti_5O_{14}$ phase appears with a homogeneous distribution. It is noticeable that an unknown phase rich in Nd and Ti formed in sample A25. It is the formation of abundant BAT phase that accumulates the barium so that the Nd–Ti phase emerged.

3.4. Grain growth of BAT phase

Fig. 5 shows the magnified backscatter electronic images of different areas in sample A10 to demonstrate the grain growth of BAT phase in the BNT solid solution. Obviously, the formation of BAT is correlated with the disappearance of $BaTi_4O_9$ and TiO_2 as follows:

$$BaTi_4O_9 + Al_2O_3 + TiO_2 \rightarrow BaAl_2Ti_5O_{14} \quad (2)$$

We consider that the aluminum goes into the structure and works in two ways. Part of it substitutes for Ti and the rest balances the charge equilibrium. With the continuous increase of Al_2O_3 to the solid solution limit, BAT grains emerge at the boundary of 3∼5 BNT grains, and then grow up gradually.

Table 2
Energy-dispersive X-ray analysis results of the crystalline phases in each BNT-A specimen.

Element	Ba/at%	Nd/at%	Ti/at%	Al/at%	O/at%	Formula
A	–	0.32	33.07	–	66.61	TiO_2
B	8.17	–	33.42	0.37	58.04	$BaTi_4O_9$
C	0.11	0.21	33.38	–	66.3	TiO_2
D	5.34	–	30.69	10.23	53.74	$BaAl_2Ti_5O_{14}$
E	5.07	–	25.72	9.82	59.39	$BaAl_2Ti_5O_{14}$
F	1.04	11.06	23.42	–	64.48	Unknown

3.5. Dielectric properties

Fig. 6 shows the dielectric constant of $Ba_4Nd_{9.33}Ti_{18}O_{54}$ ceramics with different amounts of Al_2O_3 added and sintered at different temperatures for 4 h. With the increasing of x from 0 to 2.5 wt%, the dielectric constant decreases from 82.7 to 67.7. This sharp decrease is attributed to two reasons. Firstly the substitution of Ti^{4+} ($\alpha = 2.94$ Å^3) by lower polarizability Al^{3+} ($\alpha = 0.78$ Å^3) [16] decreases the total polarizabilities thus decreased the dielectric constant. Secondly, the formation of

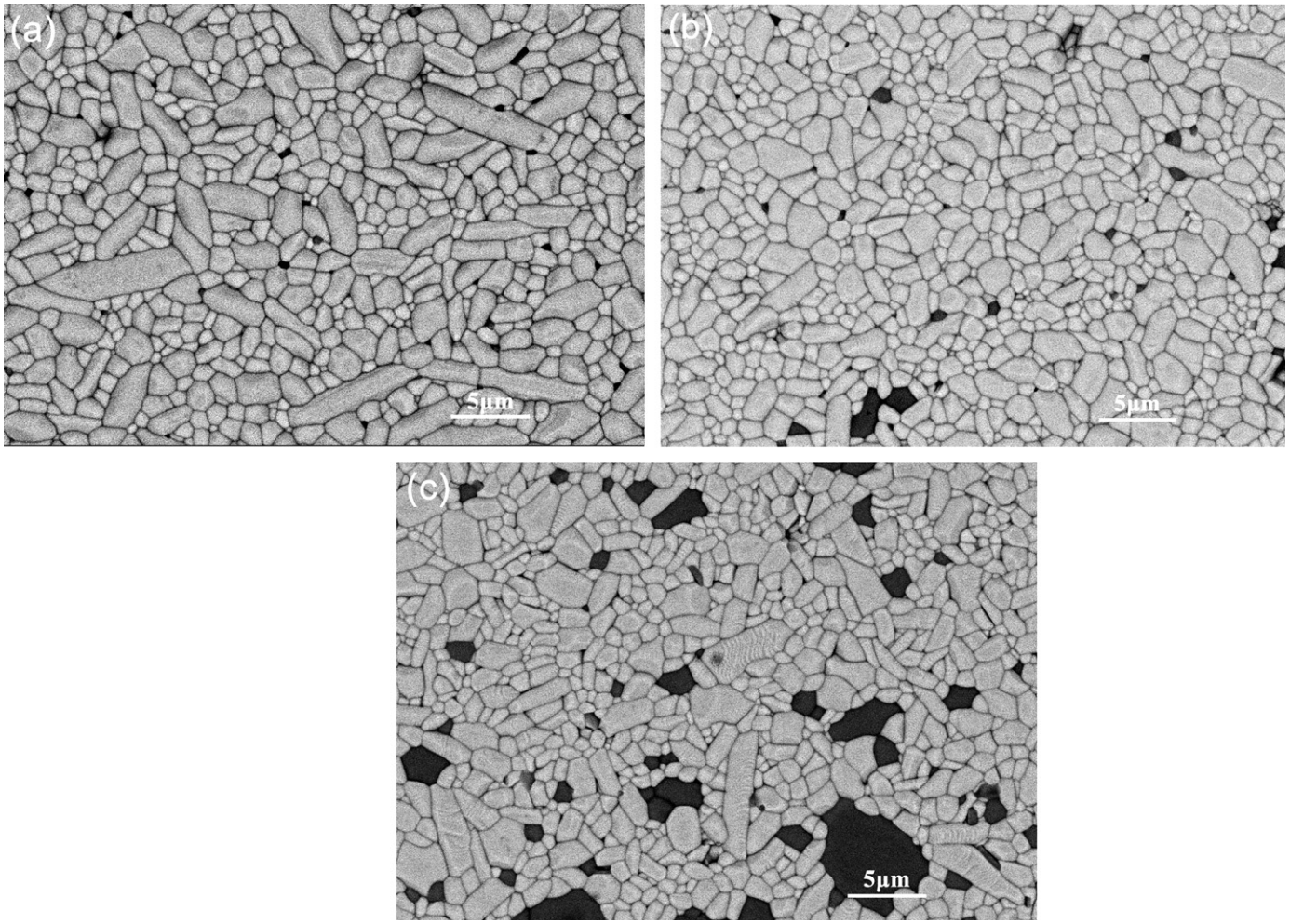

Fig. 5. Magnified backscatter electronic images of different areas in sample A10.

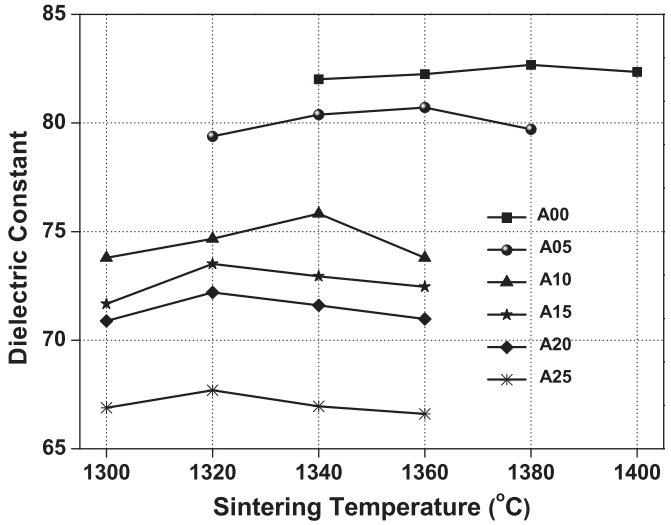

Fig. 6. Relationship between the dielectric constants of BNT-A ceramics and the sintering temperature.

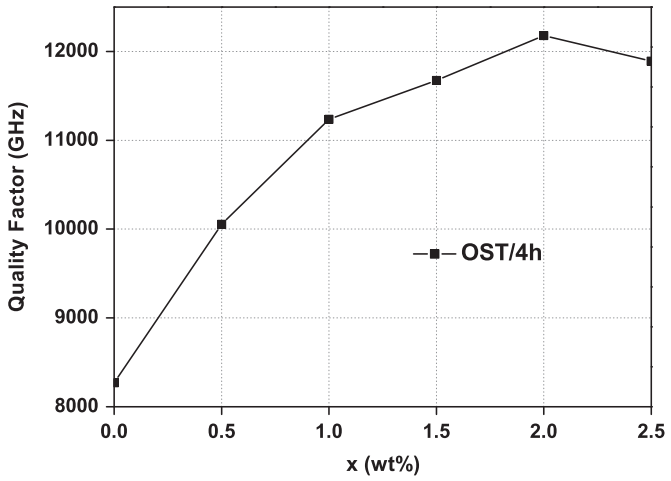

Fig. 7. $Q \times f$ values of BNT-A ceramics sintered at the optimum T_s for 4 h.

$BaAl_2Ti_5O_{14}$ phase with ε_r of 35 (tested in our previous work) decreases the total ε_r, according to the mixing rules [17].

Fig. 7 shows the $Q \times f$ values of $Ba_4Nd_{9.33}Ti_{18}O_{54}$ ceramics doped with different amounts of Al_2O_3 and sintered at the optimum T_s for 4 h. $Q \times f$ values increase with the increasing amount of Al_2O_3 to a maximum of 12,180 GHz in sample A20, and then decreased slightly. According to the discussion above, we assert that the formation of BAT phase and the homogenous distribution of it are beneficial to reduce the dielectric loss of the BNT ceramics. With BAT as the second phase, the $Q \times f$ values of BNT ceramics are greatly improved. However, the interior relation between the BAT phase and the dielectric loss of BNT ceramics is still ambiguous and needs further research.

Fig. 8 shows the temperature coefficient of resonant frequency τ_f of the $Ba_4Nd_{9.33}Ti_{18}O_{54}$ ceramics with various amounts of Al_2O_3 added and sintered at the optimum T_s for 4 h. As seen from Fig. 8, with the increase of x from 0 to 2.5, the τ_f value of the BNT ceramics decreases monotonously from 53.4 to 11.2 ppm/°C. The formation of BAT phase is believed to contribute to that change, more evidence is expected in further research.

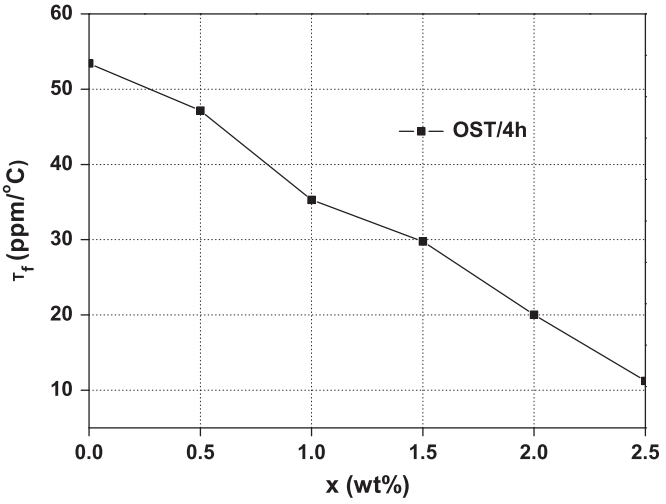

Fig. 8. Temperature coefficient of resonant frequency (τ_f) of the BNT-A ceramics sintered at the optimum T_s for 4 h.

4. Conclusions

The effects of alumina addition on the microstructure and microwave dielectric properties of $Ba_4Nd_{9.33}Ti_{18}O_{54}$ (BNT) ceramics were investigated. It was found that Al_2O_3 additive caused the formation of a second phase $BaAl_2Ti_5O_{14}$ in the material, decreasing the density and optimum sintering temperature of BNT ceramics. With increasing Al_2O_3 content from 0 to 2.5 wt%, the quality factor ($Q \times f$) of the material increased from 8270 GHz to a maximum value of 12,180 GHz and the temperature coefficient of resonant frequency τ_f decreased from +53.4 to +11.2 ppm/°C. A BNT ceramic with $\varepsilon_r = 70.2$, $Q \times f = 12{,}180$ GHz, $\tau_f = 20$ ppm/°C was obtained by adding 2.0 wt% Al_2O_3 and sintered at 1320 °C for 4 h.

References

[1] R.J. Cava, Dielectric materials for applications in microwave communications, Journal of Materials Chemistry 11 (2001) 54–62.
[2] N. Qin, X.M. Chen, Effects of Sm/Bi co-substitution on microstructures and microwave dielectric characteristics of $Ba_{6-3x}La_{8+2x}Ti_{18}O_{54}$, Materials Science and Engineering: B 111 (2004) 90–94.
[3] C.L. Huang, J.F. Tseng, Dielectric characteristics of $La(Co_{1/2}Ti_{1/2})O_3$ ceramics at microwave frequencies, Materials Letters 58 (2004) 3732–3736.
[4] C. Hoffmann, R. Waser, Hot-forging of $Ba_{6-3x}Re_{8+2x}Ti_{18}O_{54}$ ceramics (Re=La, Ce, Nd, Sm), Ferroelectrics 201 (1997) 127–135.
[5] R. Ubic, I.M. Reaney, Properties of the microwave dielectric phase $Ba_{6-3x}Nd_{8+2x}Ti_{18}O_{54}$, Ferroelectrics 228 (1999) 271–282.
[6] H. Ohsato, M. Mizuta, Microwave dielectric properties of tungsten bronze-type $Ba_{6-3x}R_{8+2x}Ti_{18}O_{54}$ (R=La, Pr, Nd and Sm) solid solution, Journal of the Ceramic Society of Japan 106 (1998) 178–182.

[7] T. Nagatomo, T. Otagiri, H. Ohsato, Microwave dielectric properties and crystal structure of the tungsten bronze-type like $(Ba_{1-\alpha}Sr_{\alpha})_6(Nd_{1-\beta}Y_{\beta})_8Ti_{18}O_{54}$, Journal of the European Ceramic Society 26 (2006) 1895–1898.

[8] J.H. Zhu, E.R. Kipkoech, W.Z. Lu, Effects of $LnAlO_3$ (Ln = La, Nd, Sm) additives on the properties of $Ba_{4.2}Nd_{9.2}Ti_{18}O_{54}$ ceramics, Journal of the European Ceramic Society 26 (2006) 2027–2030.

[9] C.C. Cheng, T.E. Hsieh, I.N. Lin, Effects of composition on low temperature sinterable Ba–Nd–Sm–Ti–O microwave dielectric materials, Journal of the European Ceramic Society 24 (2004) 1787–1790.

[10] H. Zheng, I.M. Reaney, Effect of glass additions on the sintering and microwave properties of composite dielectric ceramics based on $BaO–Ln_2O_3–TiO_2$ (Ln = Nd, La), Journal of the European Ceramic Society 27 (2007) 1787–4479.

[11] X.G. Yao, H.X. Lin, Anti-reduction of Ti^{4+} in $Ba_{4.2}Sm_{9.2}Ti_{18}O_{54}$ ceramics by doping with MgO, Al_2O_3 and MnO_2, Ceramics International 38 (2012) 3011–3016.

[12] H. Ohsato, Science of tungsten bronze-type like $Ba_{6-3x}R_{8+2x}Ti_{18}O_{54}$ (R = rare earth) microwave dielectric solid solutions, Journal of the European Ceramic Society 21 (2001) 2703–2711.

[13] B.W. Hakki, P.D. Coleman, A dielectric resonator method of measuring inductive capacities in the millimeter range, IRE Transactions on Microwave, Theory, and Techniques (1960) 402–410.

[14] F. Azough, T. Lowe, R. Freer, Control of microwave dielectric properties in the system $BaO \cdot Nd_2O_3 \cdot 4TiO_2–BaO \cdot Al_2O_3 \cdot 4TiO_2$, Journal of Electroceramics 15 (2005) 183–192.

[15] M. Mizuta, K. Uenoyama, H. Ohsato, Formation of tungsten bronze-type $(Ba_{6-3x}Sm_{8+2x})_{\alpha}Ti_{18-y}Al_yO_{54}$ ($\alpha = 1 + y/36$) solid solutions and microwave dielectric properties, Japanese Journal of Applied Physics 35 (1996) 5065–5068.

[16] R.D. Shannon, Dielectric polarizabilities of ions in oxides and fluorides, Journal of Applied Physics 73 (1993) 348–366.

[17] J.M. Wu, M.C. Chung, Reaction sequence and effects of calcination and sintering on microwave properties of $(Ba,Sr)O–Sm_2O_3–TiO_2$ ceramics, Journal of the American Ceramic Society 73 (1990) 1599–1605.